

The Development of a Thermal-Hydraulic and Nonlinear Dynamic System for Molten Salt Reactors

Asif Ali

College of Nuclear Science and
Technology
Harbin Engineering University
Harbin, China
aliasif@hrbeu.edu.cn

Yong Kuo Liu

College of Nuclear Science and
Technology
Harbin Engineering University
Harbin, China
lyk08@126.com

Waleed Raza

College of Underwater Acoustic
Engineering
Harbin Engineering University
Harbin, China
waleed@hrbeu.edu.cn

Muhammad Nazim

College of Materials Science and
Chemical Engineering
Harbin Engineering University
Harbin, China
nazimlakhan@gmail.com

Amir Ali

College of Underwater Acoustic
Engineering
Harbin Engineering University
Harbin, China
amir@hrbeu.edu.cn

Sajid Hussain

College of Nuclear Science and
Technology
Harbin Engineering University
Harbin, China
sajidhussainmailto@gmail.com

Abstract-The Molten Salt Reactor (MSR) is the most important system suggested by Generation IV for the future direction in the nuclear reactor field. For more development of the MSR reactor, the core system inside the tube is proposed by naturally circulating molten fuel salt. The nonlinear kinetic equations form a linearized function and are obtained in state-space form. Reactivity feedback and delayed neutrons are extremely important for reactor control. In this paper, a thermal-hydraulic system for the commercial computation dynamic model is proposed. Currently, there is no commercial software to simulate the natural circulation flow. The proposed method can be easily employed to detect faults and can provide a feasible overall system performance.

Keywords-molten salt reactor; thermal-hydraulic; state-space equation; delayed neutron precursor

I. INTRODUCTION

There are six reactors in Generation-IV. Among them, Molten Salt Reactor (MSR) has a unique concept that distinguishes it from the other reactor types such as light water reactors, pressure water reactors, boiling water reactors, etc. The Generation-IV reactors do not have solid nature but utilize a homogenous liquid. The benefits of the MSR and its excellent characteristics and sustainability eliminate the fuel element fabrication accurately. Therefore, high-temperature and high power density are reached in the MSR core. In the present MSR method, the circulated fuel itself is mixed with the fuel salt. Correspondingly, the reactor control mechanism or trip primary circuit may allow or produce fuel salt in the primary circuit, and circulation of the delayed-neutron precursor is generated in the core. Hence, the decay core is less important than the outer of the core [1]. The MSR is normally operated in the liquid phase because its composition tasks are affiliated with dynamic reactors. Furthermore, in the MSR operation in

steady-state, resultantly the loss of delayed neutrons affects the reactor.

In terms of modeling, MSRs are associated with solid fuel which is used in traditional reactors. Nuclear Power Plants (NPPs) are widely sophisticated systems regarding the transit and duration of modeling time. The fuel salt is always held on the outer side of the MSR core. The multiplier term for the neutron kinetics equations is added with the delayed neutron precursor [2, 3]. The MSRs are completely different from thermal-hydraulic reactor systems. In the processes of the liquid fuel failure stability of materials can be easily resolved [3]. However, a graphite zone and a thermal-hydraulic system are developed in the core [4]. In [5, 6], the fuel region is modeled as a double lasting region, which is very important in order to improve the state space equation for the outlet core temperature. In previous studies, one or two lumped parameters were applied for the thermal-hydraulic system with two lumped regions. Resultantly, the outlet core temperature is measured more accurately. The core outlet temperature is the same as the average temperature of the upper lumped region [7]. The state-action space equation is used for the reactor, thermal-hydraulic modeling, energy balance, and controls all the volume of the core and the heat exchanger (HX) unit [8]. In MSRs, when the core temperature increases, the measurement of the core outlet temperature will be inaccurate [8].

In this paper, we explore and propose a novel thermal-hydraulic method which give us more accurate and confident results without the ambiguity of the previous models.

II. THE THERMAL-HYDRAULIC METHOD

A novel thermal-hydraulic method is proposed in which a new approach has been taken to detect and resolve the problems and faults from the core outlet. In the baseline

system, an energy equilibrium equation is obtained from fuel temperature which is used without any problems in the assembled system. A maintenance equation must be described considering the core outlet temperature. In the thermal-hydraulic method, a balance equation is formed by using the control volume of the pipeline at the core outlet. Due to this distinct temperature and the insulation, the pipe section is very small (relatively to the core region). During this process, the present temperature of the core can be calculated more accurately.

The motion of delayed neutron precursors is calculated and analysis of the fuel cycle along the state action space equation is conducted. The core neutronic as well as the extended neutronic solver 1-D thermal feedbacks are acquired by the thermal-hydraulic and neutronic calculations. The thermal neutronic features of the MSR are resolved. Before the MSR fuel studies, the thermal response was known to have high neutronic in thermal-hydraulic characteristics. Hence, the obtained power distribution from the fission salt, as corresponding fuel density distribution, and the fuel salt temperature distribution throughout the core flow loop were described by the thermal-hydraulic measurement. The schematic view of the conceptual MSR is presented in Figure 1.

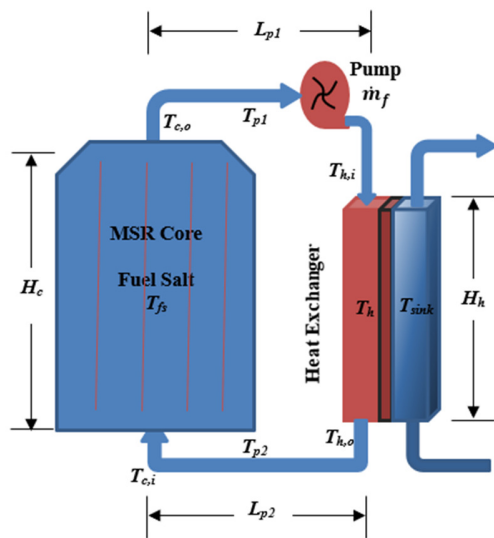


Fig. 1. Schematic representation of the MSR primary circuit.

The structure of the fast-spectrum thermal core is made by the graphite moderator elements, each of them characterized by the fast-thermal spectrum model [5, 9, 10]. The thermal spectrum liquid fuel reactor core is associated with fluoride salt and the thermal system generated a one-reserved fuel region. One circulating pump indicates the top-bottom side of the HX unit. The heat transfer mechanism is simulated with the statement of a "cooler" which operates to stabilize temperature. The heat transfer between the hot and cold sides is calculated by using the average temperature. The heat transfer coefficient is assumed to be constant [11-13].

III. MATHEMATICAL DERIVATION AND REACTOR NEUTRONS OF THE MSR

In this work, the flow effect on the liquid fuel salt and the traditional point of view of the kinetic model of the MSR core are studied and the behavior of delayed neutrons is analyzed. The acute response mechanism has been changed by the fuel density and temperature. The aggregate method has been used for fuel salt in both the reactor core and the HX unit. When more fuel salt is circulating inside the core then fission power is generated inside and outside of the core, due to the very fast delayed neutrons. The space kinetic equations derived for these regions are:

$$\frac{dp(t)}{dt} = \frac{\rho_{net}(t) - \beta_{eff}}{\Lambda} p(t) + \lambda_{eff} C(t) \quad (1)$$

$$\frac{dC(t)}{dt} = \frac{\beta_{eff}}{\Lambda} p(t) - \lambda_{eff} C(t) - \frac{1}{\tau_{core}} C(t) + \frac{e^{-\lambda_{eff}\tau_{loop}}}{\tau_{core}} C(t - \tau_{loop}) \quad (2)$$

where P and C represent the precursor concentration of the reactor power and delayed neutron precursor respectively. The terms ρ_{net} , β_{eff} , λ_{eff} , and Λ depict net reactivity and the fraction delayed neutrons emitted energy from the core. However, the various prompt neutrons per fission and the numerous delayed neutrons of precursor per fission affect the velocity of the delayed neutron decay constants of the precursor, and generation of neutron time respectively. τ shows the transit time [12]. The fuel salt passes through the core, pipe section #1, heat exchanger, and pipe section #2, and then it enters the core again as shown in Figure 1. τ_{loop} denotes the transit time outlet of the core region and it is expressed as: $\tau_{loop} = \tau_{p1} + \tau_{p2} + \tau_h$, where subscripts $p1, p2$, and h represent pipe section #1, pipe section #2, and HX respectively.

A. Neutronic Calculation Model Development

The thermodynamic characteristics of the core region are represented by the thermal power which is provided by the fuel lumped region. The average temperature of the lumped region is represented by the core fuel salt temperature. In this study, the energy balance equations are determined via an one dimension (1-D) model. The specific heat capacity is assumed to be constant and it is computed at the average temperature of the fuel. The balanced equation for the core region can be expressed as:

$$m_f c_{p,f} \frac{dT_f(t)}{dt} = p(t) - m_f c_{p,f} [T_{c,o}(t) - T_{c,i}(t)] \quad (3)$$

where m_f and \dot{m}_f show the fuel mass in the core and the fuel mass flow rate respectively, $c_{p,f}$ represents the average heat capacity of the fuel in the core, T_f , $T_{c,i}$, and $T_{c,o}$ show the core lumped fuel temperature of the moderator surface, the core inlet temperature, and the core outlet temperature [11, 14, 16].

The balanced equation for the fuel side of the HX unit is:

$$m_h c_{p,h} \frac{dT_h(t)}{dt} = m_h c_{p,h} [T_{h,i}(t) - T_{h,o}(t)] - (UA)_h [T_h(t) - T_{sink}(t)] \quad (4)$$

where m_h and \dot{m}_h represent the fuel mass in the HX and the fuel mass flow rate ($\dot{m}_h = \dot{m}_f$) respectively, $c_{p,h}$ illustrates the average heat capacity of the fuel in the HX, T_h , $T_{h,i}$, $T_{h,o}$, T_{sink}

represent the lumped fuel temperature in the HX, the inlet and the outlet temperature of the HX, and the average temperature of the heat sink. U and A_h show the overall heat transfer coefficient of the HX unit and the heat transfer area of the HX. The overall heat transfer coefficient is assumed to be constant [15, 16]. The balanced equation for pipe section #1 can be expressed as:

$$m_{p1}c_{p,p1} \frac{dT_{p1}(t)}{dt} = m_{p1}c_{p,p1} [T_{c,o}(t) - T_{h,i}(t)] - (UA)_{p1} [T_{p1}(t) - T_{\infty}] \quad (5)$$

where subscript $p1$ represents the pipe section #1, T_{p1} and T_{∞} represent the lumped fuel temperature in pipe section #1 and the ambient temperature. It is assumed that the overall heat transfer coefficient is also constant for pipe section #1.

TABLE I. MSR PARAMETERS AND RANGE OF VALUES IN THE LITERATURE

| Parameters | Symbol | Unit | Range |
|--|-----------------|--------------------------------|---|
| Reactor power | P | MWth | 400 – 4000 |
| Prompt neutron generation time | Λ | S | $10^{-6} - 10^{-7}$ |
| Initial balancing reactivity | ρ_0 | Pcm | $\beta_{eff} \left[\frac{1 - e^{-\lambda_{eff}\tau_{loop}}}{\lambda_{eff}\tau_{core} + 1 - e^{-\lambda_{eff}\tau_{loop}}} \right]$ |
| Steady-state external reactivity | ρ_{ext} | Pcm | $\rho_{ext} = -\rho_0$ |
| Effectively delayed neutron fraction | β_{eff} | - | ~ 0.00033 |
| Effectively delayed neutron decay constant | λ_{eff} | s^{-1} | ~ -0.006 |
| Core transit time | τ_{core} | S | $\sim m_f / \dot{m}_f$ |
| Loop transit time | τ_{loop} | S | $\tau_h + \tau_{p1} + \tau_{p2}$ |
| Pipe section #1 transit time | τ_{p1} | S | $\sim m_{p1} / \dot{m}_f$ |
| Pipe section #2 transit time | τ_{p2} | S | $\sim m_{p2} / \dot{m}_f$ |
| Heat exchanger transit time | τ_h | S | $\sim m_h / \dot{m}_f$ |
| Fuel temperature coefficient of reactivity | α_f | K^{-1} | $\sim -3.04 \times 10^{-5}$ |
| Fuel mass flow rate | \dot{m}_f | $kg \cdot s^{-1}$ | Depends on the power |
| Fuel mass in the core | m_f | Kg | $d_f @ T_f V_{core}$ |
| Fuel mass in the HX | m_h | Kg | $d_f @ T_h V_h$ |
| Fuel mass in the pipe section #1 | m_{p1} | Kg | $d_f @ T_{p1} V_{p1}$ |
| Fuel mass in the pipe section #2 | m_{p2} | Kg | $d_f @ T_{p2} V_{p2}$ |
| Specific heat capacity of the fuel salt | c_p | $J \cdot kg^{-1} \cdot K^{-1}$ | $-1111 + 2.782T_f$ |
| Heat exchanger heat transfer coefficient | $(UA)_h$ | $W \cdot K^{-1}$ | $P = N_{HX} (UA)_h \Delta T_{lm}^{(**)}$ |
| Average fuel temperature (in the core) | T_f | K | ~ 975 |
| Average fuel temperature (in the HX) | T_h | K | ~ 975 |
| The average temperature of the heat sink | T_{sink} | K | 750-900 |
| Ambient temperature | T_{∞} | K | ~ 3000 |
| The density of the fuel salt | d_f | $kg \cdot m^{-3}$ | $49983.56 - 0.8982T_f$ |
| The volume of the core | V_{core} | m^3 | Depends on the power |
| The volume of the HX | V_h | m^3 | Depends on the HX capacity |
| The volume of pipelines #1, #2 | $V_{p1,p2}$ | m^3 | Depends on the design |

B. Thermal Feedback Mechanism and State-Action Space

The net reactivity of the MSR can be expressed as:

$$\rho_{net}(t) = \rho_0 + \rho_{ext}(t) - \alpha_f [T_f(t) - T_{f0}] \quad (6)$$

where ρ_0 illustrates the initial balancing reactivity, ρ_{ext} represents the external reactivity which can be added with bubbles, and α_f represents the core fuel salt temperature which is changed by the graphite moderator and the reactivity coefficient. Similarly, the inlet and outlet flow rates are the same, and T_{f0} represents the steady-state fuel temperature in the core.

There is only one way to write in linear form the nonlinear differential equations considering the small perturbation around the steady-state operating point. These equations can be transformed into state-space form [16]. Around the steady-state power (P_0 and C_0), (1) and (2) can be written as:

$$\delta p(t) \frac{p_0}{dt} \delta \rho(t) + \frac{\delta \rho(t) \delta p(t) \beta_{eff}}{\Lambda} \delta p(t) + \lambda_{eff} \delta C(t) \quad (7)$$

$$\delta C(t) \frac{\beta_{eff}}{\Lambda} \delta \rho(t) - (\lambda_{eff} + \frac{1}{\tau_{core}}) \delta C(t) + \frac{e^{-\lambda_{eff} \tau_{loop}}}{\tau_{core}} \delta C(t - \tau_{loop}) \quad (8)$$

where $P(t) = P_0 + \delta P(t)$, $C(t) = C_0 + \delta C(t)$, and $\rho(t) = \delta \rho(t) = \alpha_f [T_f(t) - T_{f0}]$ due to the nature of the reactivity. The reactor has to be critical at steady-state operation, so the reference reactivity ($\rho_0 + \rho_{ext}$) will be zero at this point.

The nonlinear term, $\delta \rho(t) \delta P(t)$ still exists in (7). It can be inferred that the point kinetics equations are linear only for constant reactivity conditions. To perform linear analysis, this second-order term is neglected in this study. Lumped fuel temperatures for the core and the HX regions are calculated as:

$$T_f(t) = \frac{1}{2} [T_{c,o}(t) + T_{c,i}(t)] \quad (9)$$

$$T_h(t) = \frac{1}{2} [T_{c,o}(t) - T_{c,i}(t)] \quad (10)$$

By taking into consideration the transit times at pipe sections #1 and #2, the following substitutions:

$$T_{h,i}(t) \approx T_{c,o}(t - \tau_{p1}) \quad (11)$$

$$T_{c,i}(t) \approx T_{h,o}(t - \tau_{p2}) \quad (12)$$

can be made to state the relations between the temperatures. The temperature decrease of the fuel salt in the pipeline is neglected due to the insulation. By using (9)-(12), equations (3)-(5) can be written in the form of (13)-(15):

$$m_f c_{p,f} \dot{T}_f(t) = p_o + \delta p(t) - \dot{m}_f c_{p,h} [T_{c,o}(t) + (\tau_{p1} - \tau_{p2}) - 2T_h(t - \tau_{p2})] \quad (13)$$

$$m_h c_{p,h} \dot{T}_h(t) = 2\dot{m}_h c_{p,h} [T_{c,o}(t - \tau_{p1}) - T_h(t)] - (UA)_h [T_h(t) - T_{sink}] \quad (14)$$

$$m_{p1} c_{p,p1} \dot{T}_{c,o}(t) = \dot{m}_{p1} c_{p,p1} [T_{c,o}(t) - T_{c,o}(t - \tau_{p1})] - (UA)_{p1} [T_{c,o}(t) + T_{c,o}(t - \tau_{p1}) - 2T_\infty]/2 \quad (15)$$

where:

$$T_{p1}(t) = 1/2 [T_{c,o}(t) + T_{c,o}(t - \tau_{p1})].$$

It is assumed that $\dot{T}_{p1}(t) \approx \dot{T}_{c,o}(t)$ and that T_{sink} is constant. Finally, (7), (8), (13)-(15) take the state space form as follows:

$$\delta \dot{x} = A_1 x + A_2 x * \delta(t - \tau_{loop}) + A_3 x * \delta(t - \tau_{p1}) + A_4 x * \delta(t - \tau_{p1} - \tau_{p2}) + B \mu \quad (16)$$

where:

$$x = [\delta p(t) \delta C(t) T_f(t) T_h(t) T_{c,o}(t)]^T \quad (17)$$

$$A_1 =$$

$$\begin{bmatrix} -\frac{\beta_{eff}}{\Lambda} & \lambda_{eff} & \frac{\alpha_f p_o}{\Lambda} & 0 & 0 \\ \frac{\beta_{eff}}{\Lambda} & -\lambda_{eff} - \frac{1}{\tau_{core}} & 0 & 0 & 0 \\ \frac{1}{m_f c_{p,f}} & 0 & 0 & \frac{2\dot{m}_f}{m_f} & -\frac{\dot{m}_f}{m_f} \\ 0 & 0 & 0 & -\frac{2\dot{m}_f}{m_f} - \frac{(AU)_h}{m_f c_{p,h}} & 0 \\ 0 & 0 & 0 & 0 & -\frac{\dot{m}_f (UA)_{p1}}{m_f 2m_f c_{p,p1}} \end{bmatrix} \quad (18)$$

$$A_2 = \begin{bmatrix} 0 & 0 & 0 & 0 & 0 \\ -e^{\lambda_{eff} \tau_{loop}} / \tau_{core} & 0 & 0 & 0 & 0 \\ 0 & 0 & 0 & 0 & 0 \\ 0 & 0 & 0 & 0 & 0 \\ 0 & 0 & 0 & 0 & 0 \end{bmatrix} \quad (19)$$

$$A_3 = \begin{bmatrix} 0 & 0 & 0 & 0 & 0 \\ 0 & 0 & 0 & 0 & 0 \\ 0 & 0 & 0 & 0 & 0 \\ 0 & 0 & 0 & \frac{2\dot{m}_f}{m_f} & 0 \\ 0 & 0 & 0 & -\frac{\dot{m}_f}{m_f} - \frac{(UA)_{p1}}{2m_f c_{p,p1}} & 0 \end{bmatrix} \quad (20)$$

$$A_4 = \begin{bmatrix} 0 & 0 & 0 & 0 & 0 \\ 0 & 0 & 0 & 0 & 0 \\ 0 & 0 & 0 & 0 & -\frac{\dot{m}_f}{m_f} \\ 0 & 0 & 0 & 0 & 0 \\ 0 & 0 & 0 & 0 & 0 \end{bmatrix} \quad (21)$$

$$\beta = \begin{bmatrix} -\frac{\alpha_f p_o}{\Lambda} & 0 & 0 & 0 & 0 \\ 0 & 0 & \frac{1}{m_f c_{p,f}} & 0 & 0 \\ 0 & 0 & 0 & \frac{(UA)_h}{m_f c_{p,h}} & 0 \\ 0 & 0 & 0 & 0 & \frac{(UA)_{p1}}{m_f c_{p,p1}} \end{bmatrix}^T \quad (22)$$

$$u = [T_{f0} \ P_0 \ T_{sink} \ T_\infty]^T \quad (23)$$

It is important to note that $\dot{m}_f = \dot{m}_h = \dot{m}_{p1} = \dot{m}_{p2}$ due to the closed-loop operation (the variation of the expansion tank level is neglected). All physical properties were taken as constant and were calculated at the average temperature of the lumped regions. Calculated transit time can be divided into to the length of system (or height) by the velocity of the fluid.

IV. RESULTS AND DISCUSSION

In this section, the results of the numerical analysis for the proposed system are presented. The primary loop of MSR is simulated under the steady state in Matlab/Simulink. When the fuel pump rotation decreases in the start of transient, the primary flow will reduce within a few seconds. Furthermore, the reactor core fraction of the delayed neutron precursors will increase because they have the tendency to improve the reactivity and the reactivity loss due to the fuel lumped temperature. Therefore, heat is produced by fuel lumped temperature in the reactor core, so that the temperature difference between core inlet and core outlet is increased in the dynamic model as shown in Figure 2.

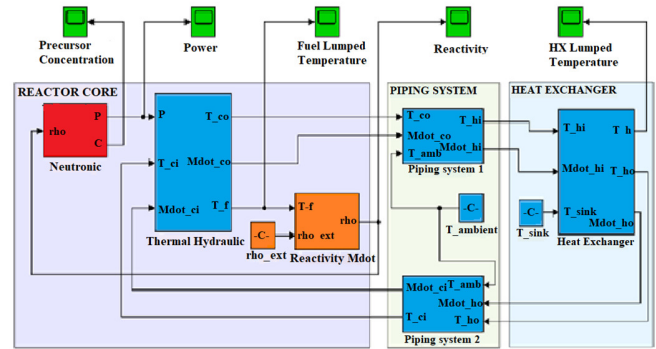


Fig. 2. Simulink model.

The core dynamic model is associated with the neutronic and thermal-hydraulic coupled system. Coupling is obtained by the reactivity feedback mechanism. In this device, the input components are outer reactivity, ambient temperature, and heat sink temperature. The output values are the reactor power and the core outlet temperature. The simulation parameters are given in Table II.

Several different MSR concepts have been presented. Therefore, there is a wide variety of values for both input and output parameters. The module "1" presents the MSR (fast or thermal) parameters and their range value can be used for the developed model and tool.

TABLE II. MSR PARAMETERS USED IN THE SIMULATION

| Parameter | Value |
|--|-----------------------|
| Reactor power | 4000MWth |
| Average core temperature | 700°C |
| Core transit time | 2s |
| Loop transit time | 2s |
| Transit time for each pipe | 0.1s |
| Effectively delayed neutron fraction | 0.0033 |
| Effectively delayed neutron decay constant | 0.0611s ⁻¹ |
| Prompt neutron generation time | 0.95e-6s |
| Fuel temperature coefficient of reactivity | 3.4e-5K ⁻¹ |
| Coolant bulk temperature | 570°C |
| Ambient temperature | 40°C |

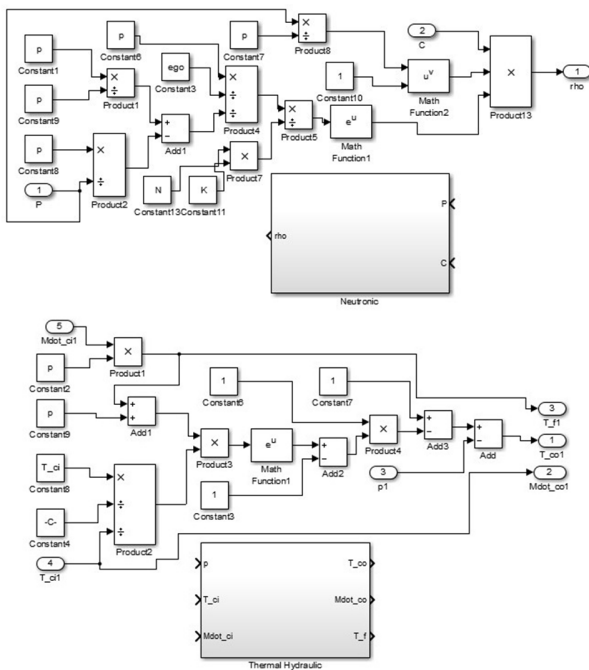


Fig. 3. The sub model of neutronic and thermal hydraulic.

Three sub models of the Simulink model are used to describe the Simulink model shown in Figure 2 representing three individual parts of the Simulink model. Figure 3 shows the neutronic and thermal-hydraulic sub model. It is used to diagnose faults from the core and give information about the fuel salt temperature distribution from the core. Figure 4 shows the reactivity model and the piping system #1 of the MSR. Therefore it shows the lumped fuel temperature and it represents all constant transfer temperatures in the piping system, while fuel salt passes through piping system #1. Figure 5 represents the piping system #2 and the HX of the MSR. It shows the heat capacity inlet and outlet temperature of the HX. Figure 6 shows the thermal reactor which reached the 3.02GW equilibrium by using the parameters illustrated in Table I. The reactor reached the steady-state equation level at 100s. The fuel temperature changes between the HX region and the core region, because temperature is reduced due to the loss of the pipeline of the heat by 1°K. The fuel temperature increased by 100°K in the reactor transverse core. These features can be used in the perturbation system.

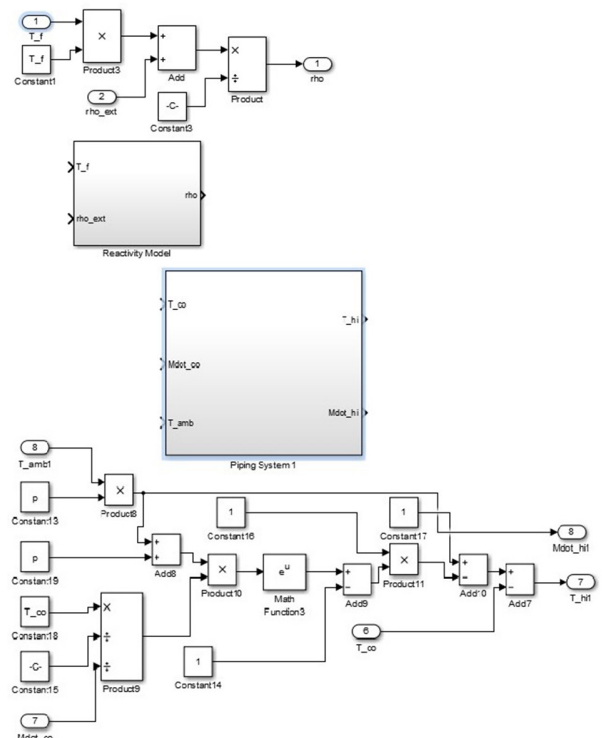


Fig. 4. The sub model of the reactivity model and piping system #1.

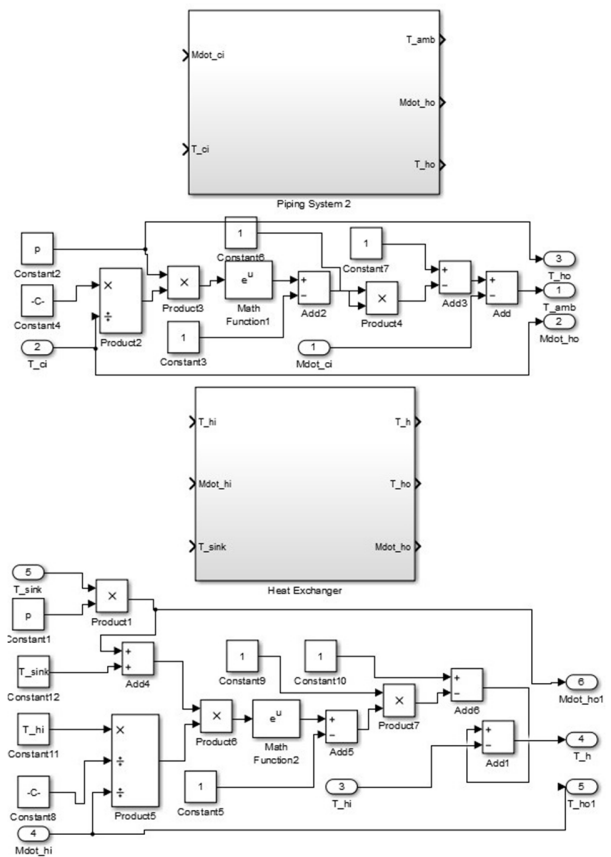


Fig. 5. The sub model of the piping system #2 and the HX.

The proposed model's derived state-space equations can be used for any specific fast MSR. The equations are written for generic parameters. The fuel temperature variance between the core region and the HX region is very small, due to the 1°K temperature decrease because of the losses of heat at the pipelines. In this type of reactor, temperature of 100°K is developed transversely in the core. The MSRs can be simulated with the proposed model. This feature can also be applied into perturbation cases. The components of the reactor system are adopted from the literature.

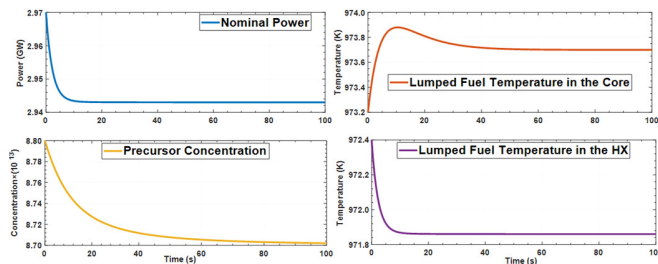


Fig. 6. Reactor parameters at steady-state operation.

V. CONCLUSION

Many dynamic methods considering the thermal MSR have been presented in previous works. In this paper, we used two or more lumped regions at the reactor core for the thermal-hydraulic modeling. It was assumed that the outlet core temperature is the same as the average temperature of the higher lumped region. The outlet core temperature is measured inaccurately due to the high temperature at the core reactor. For all types of MSR, measuring the fast spectrum or thermal fuel types is very important. There are no distinct dynamic methods for the fuel position in the core. The methods regarding other positions of the thermal reactor have significant differences that are caused by the moderator region. Considering the feedback effects, the moderator temperature of the graphite region has been modeled in the thermal MSRs, even though there is no concept of the moderator region in the fast MSR.

A new kinetic method has been proposed for fast MSRs in this paper. There is only one lumped region that has been assumed for the reactor core, which has only fuel salt. Therefore, energy has been balanced for the outlet core temperature that is described using pipeline temperature. The steady-state operation of MSR, the nonlinear kinetic equation, the Matlab/Simulink system, and the state-space model have been presented. The new model was tested in simulations and the conclusion is that the conceptual reactor can be used in real applications.

ACKNOWLEDGMENT

The authors would like to thank the Natural Science Foundation of Heilongjiang Province, China (Grant No. A2016002), the Foundation of Science and Technology on Reactor System Design Technology Laboratory (HT-KFKT-14-2017003), the technical support project for Suzhou Nuclear Power Research Institute (SNPI) (No.029-GN-B-2018- C45-P.0.99-000 03), and the Research Institute of Nuclear Power

Operation (No. RIN180149-SCCG) for funding this research project.

REFERENCES

- [1] C. Yu *et al.*, "Th-U breeding performance in a Channel-type molten salt Fast reactor with different starting fuels," *Annals of Nuclear Energy*, vol. 122, pp. 91–100, Dec. 2018, <https://doi.org/10.1016/j.anucene.2018.08.003>.
- [2] V. Singh, "Study of the Dynamic Behavior of Molten-Salt Reactors," M. S. thesis, University of Tennessee, Knoxville, TN, USA, 2019.
- [3] D. Suescún-Díaz and G. Espinosa-Paredes, "On the numerical solution of the point reactor kinetics equations," *Nuclear Engineering and Technology*, vol. 52, no. 6, pp. 1340–1346, Jun. 2020, <https://doi.org/10.1016/j.net.2019.11.034>.
- [4] V. V. Ignatiev *et al.*, "Molten-salt reactors: new possibilities, problems and solutions," *Atomic Energy*, vol. 112, no. 3, pp. 157–165, Jul. 2012, <https://doi.org/10.1007/s10512-012-9537-2>.
- [5] V. Singh, M. R. Lish, A. M. Wheeler, O. Chvála, and B. R. Upadhyaya, "Dynamic Modeling and Performance Analysis of a Two-Fluid Molten-Salt Breeder Reactor System," *Nuclear Technology*, vol. 202, no. 1, pp. 15–38, Apr. 2018, <https://doi.org/10.1080/00295450.2017.1416879>.
- [6] A. Asif *et al.*, "Advancement of Integral Fast Reactor," *Journal of Applied and Emerging Sciences*, vol. 10, no. 2, pp. 149–154, Dec. 2020, <https://doi.org/10.36785/jaes.v10i2.453>.
- [7] J. Stewart, "Gen-Foam Multiphysics Model Development for Molten Salt Reactors," Ph.D. dissertation, University of Nevada, Las Vegas, NV, USA, 2020.
- [8] A. M. Leandro, F. Heidet, R. Hu, and N. R. Brown, "Thermal hydraulic model of the molten salt reactor experiment with the NEAMS system analysis module," *Annals of Nuclear Energy*, vol. 126, pp. 59–67, Apr. 2019, <https://doi.org/10.1016/j.anucene.2018.10.060>.
- [9] B. Mignacca and G. Locatelli, "Economics and finance of Molten Salt Reactors," *Progress in Nuclear Energy*, vol. 129, p. 103503, Nov. 2020, <https://doi.org/10.1016/j.pnucene.2020.103503>.
- [10] Y. Kassem, H. Camur, and O. a. M. Abughinda, "Solar Energy Potential and Feasibility Study of a 10MW Grid-connected Solar Plant in Libya," *Engineering, Technology & Applied Science Research*, vol. 10, no. 4, pp. 5358–5366, Aug. 2020, <https://doi.org/10.48084/etasr.3607>.
- [11] C. Shi, M. Cheng, and G. Liu, "Development and application of a system analysis code for liquid fueled molten salt reactors based on RELAP5 code," *Nuclear Engineering and Design*, vol. 305, pp. 378–388, Aug. 2016, <https://doi.org/10.1016/j.nucengdes.2016.05.034>.
- [12] Z. Zou, C. Shen, X. Zhang, S. Wang, and H. Chen, "3D thermal hydraulic characteristics analysis of pool-type upper plenum for lead-cooled fast reactor with multi-scale coupling program," *Nuclear Engineering and Design*, vol. 370, Dec. 2020, Art. no. 110892, <https://doi.org/10.1016/j.nucengdes.2020.110892>.
- [13] A. Asif *et al.*, "Recent Advances in Nuclear Power Plant for Fault Detection and Diagnosis - A Review," *Journal of Critical Reviews*, vol. 7, Dec. 2020, Art. no. 10, <https://doi.org/10.31838/jcr.07.18.535>.
- [14] P. Zhao, Z. Liu, T. Yu, J. Xie, Z. Chen, and C. Shen, "Code development on steady-state thermal-hydraulic for small modular natural circulation lead-based fast reactor," *Nuclear Engineering and Technology*, vol. 52, no. 12, pp. 2789–2802, Dec. 2020, <https://doi.org/10.1016/j.net.2020.05.023>.
- [15] B. Doğan and T. Ölmez, "A novel state space representation for the solution of 2D-HP protein folding problem using reinforcement learning methods," *Applied Soft Computing*, vol. 26, pp. 213–223, Jan. 2015, <https://doi.org/10.1016/j.asoc.2014.09.047>.
- [16] R. Yoshioka, Y. Shimazu, and K. Mitachi, "Guidelines for MSR Accident Analysis," presented at the Thorium Energy Conference, Shanghai, China, 2013.